Elsevier Editorial System(tm) for Journal of Molecular Structure
Manuscript Draft

Manuscript Number: RF2014_4364R1

Title: A joint experimental and theoretical study on the electronic structure and photoluminescence properties of Al2(WO4)3 powders

Article Type: Research Paper

Keywords: Al2(WO4)3; Electronic structure; Clusters; DFT calculations; Photoluminescence

Corresponding Author: Prof. Laécio Santos Cavalcante, Prof. Dr.

Corresponding Author's Institution: Universidade Federal de São Carlos-UFSCar

First Author: Francisco Marcos C Batista, Ms.

Order of Authors: Francisco Marcos C Batista, Ms.; Felipe A la Porta, Dr.; Lourdes Gracia, Dr.; Elena Cerdeiras, Dr.; Lourdes Mestres, Prof. Dr.; Maximo S Li, Prof. Dr.; Nouga C Batista, Prof. Dr.; Juan Andres, Prof. Dr.; Elson Longo, Prof. Dr.; Laécio Santos Cavalcante, Prof. Dr.

Response to Reviewer Comments#RF2014-4364R1

Manuscripts with Decisions: ***Revise***

Title: ***A joint experimental and theoretical study on the electronic structure and photoluminescence properties of $Al_2(WO_4)_3$ powders***

Journal: ***Journal of Molecular Structure***

Dear Editor (***Prof. PHD. Rui and Editorial Office "Elsevier"***) and **Reviewer#1.** The revised version of the manuscript presents the additional changes and suggested comments in **bold** in the manuscript.

Reviewers' comments:

Reviewer#1: RF2014-4364R1

The presented paper "A joint experimental and theoretical study on the electronic structure and photoluminescence properties of $Al_2(WO_4)_3$ powders" by L.S. Cavalcante et al. includes 12 pages, 1 table, 6 figures and 53 reference items. The work is interesting and discerning especially for optical properties of examined tungstates compounds. The manuscript reports synthesis, electronic structure and photoluminescence (PL) properties of $Al_2(WO_4)_3$ powders obtained by a two-step synthetic route based on the co-precipitation method which was followed the by a calcination process at different temperatures. These powders were structurally and morphologically characterized by means of X-ray diffraction (XRD), Rietveld refinement and field emission scanning electron microscopy (FE-SEM). Optical properties were investigated by ultraviolet-visible (UV-vis) absorption spectroscopy and photoluminescent measurements at room temperature. Stable electronic excited states (singlet) have been characterized by using DFT method at the B3LYP calculation level of model.

Answer – The merits and the novelty of the work are related to literature has not yet presented theoretical data in electronic excited states (singlet) for this material.

Obtained results offers new ideas and perspectives on the behavior of photoluminescent materials and the results suggest that these materials are promising for applications in photovoltaic devices and catalysis.

Answer – We are still delving into this material and a future work with nano and micro crystals obtained by microwave heating and its photocatalytic properties will reported at next year.

Therefore to obtain some work benefits will be enforcing few changes which will also constitute for its quality. There are following remarks and proposal:

1º) I pointed out that in the paper there is lack of Experimental Section (Materials and Methods). I suggest that the instrumental information should be moved from the body of the text to the mentioned section. Please re-edit the manuscript.

Answer – We have improved the part related to English grammar of the all manuscript.

2º) P.4 In my opinion, the equations 1 and 2 are obvious. They should be removed.

- P. 6, row: 6; The dash should be deleted. rows 15,

Answer – I agree with the opinion of Reviewer#1. Therefore, we have deleted the equation (1) and (2). In addition the equation (3) was adjusted of form more clearly to readers of the Journal of Molecular Structure.

3º) The following sentence is not clear and is too complicated

- P.7, rows 2-3;

Answer – Dear Reviewer#1, you're right we have improved completely this phrase and improved explanations of the Rietveld refinement, modeling of the unit cell and added 2 fundamentals references to clarify the modeling of clusters.

4º) It should be point out the temperature at which the Rietveld analysis was treated. rows 11-13.

Answer – We have added this information in abstract, text and supplementary data (Table S2). Moreover, we have improved a new refinement Rietveld data (R_p; R_{exp}; R_{wp}; χ^2; and GoF) and Figure S2.

5º) The details of octahedral and tetrahedral geometry are known. Please delete the information inside the parentheses. rows 15-17

Answer – We have removed this basic information inside the parentheses of our manuscript.

6º) The following sentence is unclear.

- P. 11, rows 17-21.

Answer – We have improved the part related to English grammar of the all manuscript.

7º) The following sentence is not clear and is too complicated.

- P. 12, rows 15-19.

Answer – We have improved the part related to English grammar of the all manuscript.

8º) The sentence is too long and unclear.- Table 1;

Answer – We have improved the part related to English grammar of the all manuscript.

9º) The values of bond angles mentioned in the text are missing. There are also lack of units of distances and cell parameters. Please complete this data.

Answer – We added this information in Table S2. Moreover, we have improved a new refinement Rietveld data (R_p; R_{exp}; $R_{wp;}$ χ^2; and GoF).

10º) Generally, several grammatical mistakes in the manuscript are appeared and I recommend revision of the manuscript by an English native speaker.

Answer – We have improved the part related to English grammar of the all manuscript.

11º) I recommended publishing the paper in Journal of Molecular Structure after these corrections.

Dear Reviewer#1: "Thank you for their valuable comments. We believe that all corrections are necessary and very important to improve the quality of our manuscript."

Sincerely,

Prof. Dr. ***Laécio Santos Cavalcante***

CCN-DQ-GERATEC, Universidade Estadual do Piauí, João Cabral, Nº. 2231, P.O. Box 381, ZIP: 64002-150, Teresina-PI, Brazil;

Phone: +55 (16) 3301-6643 Mob: +55 016 8127-9158;

Emails: laeciosc@gmail.com or laeciosc@bol.com.br

Currículo Lattes: http://lattes.cnpq.br/7690248628577122

A joint experimental and theoretical study on the electronic structure and photoluminescence properties of $Al_2(WO_4)_3$ powders

F.M.C. Batista[a], F.A. La Porta[b,c], L. Gracia[b,c], E. Cerdeiras[a], L. Mestres[a], M. Siu Li[d], N.C. Batista[e], J. Andrés[b], E. Longo[c], L.S. Cavalcante[e*]

[a]*Departament de Química Inorgànica, Facultat de Química, Universitat de Barcelona, 08028 Barcelona, Spain*
[b]*Departament de Química Física i Analítica, UJI – Universitat Jaume I, Av. de Vicent Sos Baynat, s/n, Castelló de la Plana, 12071, Spain*
[c]*Universidade Estadual Paulista, P.O. Box 355, 14801-907, Araraquara-SP, Brazil*
[d]*IFSC-Universidade de São Paulo, P.O. Box 369, 13560-970, São Carlos, SP, Brazil*
[e]*CCN-DQ-GERATEC, Universidade Estadual do Piauí; João Cabral, N. 2231, P.O. Box 381, CEP: 64002-150, Teresina-PI, Brazil*

Abstract

In this paper, aluminum tungstate $Al_2(WO_4)_3$ powders were **synthesized** by the co-precipitation method **at room temperature** and **then submitted to heat treatment** process at different temperatures **(100, 200, 400, 800, and 1000ºC)** for 2 h. **The structure and morphology of powders were characterized by means of** X-ray diffraction **(XRD)**, **Rietveld refinement data**, and field emission scanning electron microscopy **(FE-SEM)** images. Optical properties were investigated by ultraviolet−visible **(UV-vis) diffuse reflectance** spectroscopy and photoluminescence **(PL)** measurements. **XRD patterns and Rietveld refinement data showed that $Al_2(WO_4)_3$ powders heat treated at 1000ºC for 2 h have a orthorhombic structure with a space group (*Pnca*) without the presence of deleterious phases. FE-SEM images reveals these powders are formed by aggregation of several nanoparticles leading to growth of microparticles with irregular morphologies and agglomerated nature. UV-vis spectra indicated the increase in the optical band gap energy from 3.16 to 3.48 eV) with rise of processing temperature, which is associated with the reduction of intermediary energy levels.** First-principles calculations were performed by density functional theory at the B3LYP calculation on periodic model systems point out that the presence of stable electronic excited states (singlet), **in order to understand the behavior of the PL properties.** The **analyses** of the band structures and density of states **to** both ground and first excited electronic states provides a deep insight on the main features based on structural and electronic order-disorder effects **in** octahedral [AlO_6] clusters **and** tetrahedral [WO_4] clusters, as constituent building units of this material.

Keywords: $Al_2(WO_4)_3$; Electronic structure; Clusters; DFT calculations; Photoluminescence

*Tel: +55 86 3351 8111, Mob: +55 86 9808 4129. *Email address:* laeciosc@bol.com.br (L.S. Cavalcante*)

1. Introduction

Aluminum tungstate $Al_2(WO_4)_3$ **is an important semiconductor material** belonging to the family of trivalent tungstates compounds with **general formula** $\boldsymbol{X}_2(WO_4)_3$, where [$\boldsymbol{X}$ = Y^{3+}, Sc^{3+}, In^{3+}, Al^{3+} **and rare earths as lanthanides** (Ho to Lu)]. **This oxide has attracted wide interest of several researchers due to excellent physical and chemical properties** [1–9]. **Moreover,** $Al_2(WO_4)_3$ presents an orthorhombic structure with *Pnca* space group [10,11], in which a larger pore framework structure formed by octahedral [AlO_6] clusters and tetrahedral [WO_4] clusters can be sensed. These building blocks can be considered the constituent clusters of this system, and they connected in such a manner that they form a layered structure with a large tunnel size, where the Al^{3+} cations are **sufficiently** mobile.

In the last years, different synthetic methods such as co-precipitation (CP) [12,13], sol–gel [14], modified Pechini [15], solid state reaction [16], **and** Czochralski **crystal growth** [17] have been used to obtain $Al_2(WO_4)_3$ crystals. In addition, doping processes of metals (Eu^{3+}, Cr^{3+}, and Yb^{3+}, etc) on this material generate excellent waveguides for spectroscopy [16], luminescence properties [18], and broad band laser [19]. These doping processes provoke a change in the lattice parameters as function of both ionic charge and radius, and then, there is an alteration of electronic properties due the ionic conductivity into the orthorhombic structure [12]. In particular, negative thermal expansion (NTE) is the most commonly electronic property studied for this compound [20–25]. The NTE behaviour in this material is **associated** to the presence of low frequency rigid modes facilitated by their open network structure with corner linking octahedral **[AlO_6]** and tetrahedral **[WO_4]** clusters [6,24]. Theoretical investigations show a close relation between pressure induced amorphization and NTE in these tetrahedral bonded network structures [26]. Moreover, the high pressure behaviour of NTE ceramics materials is also of significant current interest in basic sciences to temperature sensor [20].

Therefore, in this paper, we report for the first time the synthesis, electronic structure and photoluminescence (PL) properties of $Al_2(WO_4)_3$ powders obtained by a two-step synthetic route based on the CP method which was followed the by a calcination process. These powders were structurally and morphologically characterized by means of X-ray diffraction (XRD), Rietveld refinement and field emission scanning electron microscopy (FE-SEM). Optical properties were monitored by ultraviolet-visible (UV–vis) **diffuse reflectance** spectroscopy and PL measurements at room temperature. Clusters concept have been used by our group as a basic units of a given crystal [27–29], and in the present case, the different forms that are organized inside the $Al_2(WO_4)_3$ crystal structure, i.e. octahedral [AlO_6] **clusters** and tetrahedral [WO_4] clusters, play a key role on their physical and chemical properties. The subtle balance between the electronic order-disorder effects and distortions in clusters reflected in optical properties of $Al_2(WO_4)_3$ crystal have been addressed by first principles calculations by using the density functional theory (DFT) at the B3LYP calculation level in order to provide a framework for the interpretation of experimental data.

2. Experimental details

2.1. Synthesis of $Al_2(WO_4)_3$ powders by the CP method

$Al_2(WO_4)_3$ powders were prepared by the CP method at room temperature without surfactant in aqueous solutions. The typical $Al_2(WO_4)_3$ powder synthesis procedure is described as follows: 3×10^{-3} mols of tungstate (VI) sodium dihydrate [$Na_2WO_4.2H_2O$] (99% purity, Panreac) and 2×10^{-3} mols of aluminum nitrate nonahydrate [$Al(NO_3)_3.9H_2O$] (99% purity, Sigma-Aldrich) were dissolved separately in two plastic tubes (Falcon) with 50 mL of deionized water in each tube. The first solution with $\mathbf{6}Na^{+}$ and $\mathbf{3}\,WO_4^{2-}$ ions was transferred to a **PYREX glass beaker with capacity of 250 mL** under constant stirring for 2 min. The second solution with ($\mathbf{2}Al^{3+}$ and $\mathbf{6}\,NO_3^{-}$) ions **was added to this system where a white**

suspension is rapidly formed. In aqueous solutions, the fast reactions between $2Al^{3+}$ and $3\,WO_4^{2-}$ ions is due to force of electrostatic attraction, which resulted in the formation of amorphous or disordered $Al_2(WO_4)_3$ precipitates.

2.2. Calcination of amorphous $Al_2(WO_4)_3$ powders obtained by the CP method

The resulting suspensions were washed with deionized water several times to remove all Na^+ ions. The powders were then heat-treated at 100°C, 200°C, 400°C, 800°C and 1000°C for 2 h. The chemical reactions between $2Al^{3+}/3\,WO_4^{2-}$ ions and solid state at different temperatures promote a phase transformation from an amorphous state to a crystalline and/or structural transition from disordered to ordered lattice, as shown in equations (1).

$$2Al^{3+}_{(aq)} + 3WO^{2-}_{4(aq)} \xrightarrow{25^{o}C} Al_2(WO_4)_{3(s)} \xrightarrow{100,200,400^{o}C} Al_2(WO_4)_{3(s)disordered} \xrightarrow{800,1000^{o}C} Al_2(WO_4)_{3(s)ordered} \ldots\ldots (1)$$

Finally, these white color $Al_2(WO_4)_3$ powders were structurally and morphologically characterized by different techniques.

2.3. Characterizations of $Al_2(WO_4)_3$ powders

$Al_2(WO_4)_3$ powders were structurally characterized by XRD patterns using a X'Pert PRO MPD Alpha1 (PANalytical, USA) with Cu–Kα radiation (λ = 1.5406 Å) in the 2θ range from 5° to 80° in the normal routine with a scanning velocity of 2°/min and from 10° to 110° with a scanning velocity of 0.5°/min of a 0.02º step in the Rietveld routine. Thermogravimetric analysis (TGA), differential thermogravimetric analysis (DTA) and differential scanning calorimetry (DSC) were performed using a SDT Q600 (TA instruments, USA) from room temperature to 1200ºC with a heating rate of 5ºC/min. The shapes and sizes of these $Al_2(WO_4)_3$ powders were observed **using** a FE-SEM model Inspect F50 (FEI Company, Hillsboro, OR) operated at 15 kV. UV−vis spectra were taken using a Varian

spectrophotometer (model Cary 5G) in a diffuse-reflectance mode. PL measurements were performed at room temperature through a Monospec 27 monochromator (Thermal Jarrel Ash) coupled to a R446 photomultiplier (Hamamatsu Photonics, Japan). A krypton-ion laser (Coherent Innova 90K; λ = 350 nm) was used as the excitation source; its maximum output power was maintained at 500 mW. The laser beam was passed through an optical chopper, and its maximum power on the sample was maintained at 40 mW. All the measurements were performed at room temperature.

2.4. Theoretical methods and model systems

All calculations were performed by using the DFT method with the B3LYP hybrid functional [30,31], as implemented in the CRYSTAL 09 computer code [32]. The large-core ECP basis derived by Hay and Wadt [33], the ECP68 has been chosen for W atoms, and the Al and O **atoms** are described with an all-electron by 9763-311(d631)G* for Al and 6-31G* for O atoms, respectively [34]. The level of accuracy for the Coulomb and exchange series was controlled by five thresholds set to (10^{-6}, 10^{-6}, 10^{-6}, 10^{-6}, and 10^{-12}). The shrinking (Monkhorst–Pack) [35] factor was set to 6, which corresponds to 80 independent k-points in the irreducible part of the Brillouin zone integration.

Based on the experimental refinement of the **XRD results and Rietveld refinement data** presented in this research, two periodic models were used to find the singlet ground (***s***) and excited singlet electronic states (***s****). These models can be useful to represent different structural and electronic order-disorder effects in the material. An excited state is obtained by imposing a low and high spin state that must promote an electron from the valence band (VB) to the conduction band (CB). However, it is important to remark that accurate excited electronic states calculation of periodic systems still represents a challenge for quantum-chemical methods [36]. This methodology has been previously employed by us to show how

the structural disorder affects the band gap value, in particular to understand the transitions associated to PL emission behavior of perovskite (ABO_3) [37,38], tungstate (AWO_4) [39] and molybdate ($AMoO_4$) based materials [40]. Per unit cell, this implies to impose two electrons with the opposite or same spin, corresponding to the singlet and triplet electronic state, respectively. It also creates **Frenkel excitons** (**holes** in the VB, **electrons** in the CB). In the present case, any attempt to find excited states with triplet mutiltiplicity was unsuccessfully. To confirm the character of local minima on potential energy surfaces, vibrational frequency calculations were carried out to ensure that there are only positive frequencies which correspond to minima for both ground and excited singlet electronic states. The analysis of the results was performed by the calculation of the density of states (DOS), band structure, charge **density** and band gap value. The XcrysDen program [41] was used for the band structure drawing design.

3. Results and discussion

3.1. XRD patterns analyses

Fig. 1(a–e) shows XRD patterns for $Al_2(WO_4)_3$ powders obtained by **the CP method** and heat-treated at different temperatures for 2 h.

<Fig. 1(a–e)>

An analysis of the results renders that the as-**synthesized** powders at 100ºC, 200 ºC, and 400ºC for 2 h did not exhibit diffraction peaks; then they a**re amorphous or structurally disordered** at long range (see Figs. 1(a–c)). Moreover, we have accompanied the decomposition process of amorphous precursor powder by TGA analysis evolution and DTA. The TGA and DTA curves we observed water loss at about 145ºC and our results indicate that

the temperature required to crystallize $Al_2(WO_4)_3$ powders is 600ºC (see Supplementary data; Figs S1(a,b)). In general, $Al_2(WO_4)_3$ powders heat–treated at 800ºC and 1000ºC for 2 h exhibited all diffraction peaks related to the pure phase which can be indexed perfectly to a orthorhombic structure with a space **group** (*Pnca*) **with** four molecular formula per unit cell (Z = 4) and a respective inorganic crystal structure database (ICSD; N^o. 90936) [42].

3.2. Structural representation of $Al_2(WO_4)_3$ crystals

Fig. 2 illustrates a schematic representation for orthorhombic $Al_2(WO_4)_3$ unit cells modeled from Rietveld refinement data **of $Al_2(WO_4)_3$ powders heat–treated at 1000ºC for 2 h.**

<Fig. 2>

This unit cell illustrated in Fig. 2 was obtained by means of Rietveld refinement data to system more organized. The lattice parameters, unit cell volume, atomic coordinates and site occupation were obtained and calculated using the Rietveld refinement method [43], using the ReX Powder diffraction program version 0.7.4 [44]. Moreover, the Rietveld refinement data were used to model these unit cells using the Visualization for Electronic and Structural Analysis (VESTA) program, version 3.2.1, for Windows64bit [45]. These data are listed and illustrated in the (Supplementary data file; Table S1 and Figs S2). This unit cell illustrated in Fig. 2 is assigned to an orthorhombic structure of $Al_2(WO_4)_3$ crystals, which is characterized by exhibiting a space group *Pnca* and four molecular formula per unit cell (Z = 4) [**46**]. In these unit cells, basically the Al atoms are coordinated to six O atoms which form the distorted octahedral [AlO_6] clusters, while **the** W

atoms are coordinated to four O atoms which form [WO_4] clusters with a tetrahedral polyhedral configuration, which are illustrated in Fig. 2.

In particular, refinement results point out that the tetrahedral [WO_4] clusters are highly distorted in the lattice and exhibit a particular characteristic related to differences in the O–W–O bond angles. There are two types of [WO_4] clusters: [$W1O_4$] and [$W2O_4$], being the latter more distorted than the former (Supplementary data Figs S3). This result can be related to the experimental conditions required to obtain pure $Al_2(WO_4)_3$ crystals. FE-SEM images revealed large particles of crystalline $Al_2(WO_4)_3$ powders with irregular shapes (see Supplementary data; Figs S4(a–e)). In particular, the random aggregation process between the small particles results in the formation of irregular-shaped crystallites. We believe that particle growth is related to mass transport mechanisms via nanocrystalline particle diffusion during the sintering process by an increase of the heat treatment. Although a detailed mechanistic study goes beyond the scope of this work, and will be subject of future investigations.

Table 1 shows the values for the optimized Al–O and W–O distances and O–W–O bond angles for the ground singlet (***s***) and excited singlet (***s****) electronic states.

<Table 1>

The calculated distance values between W–O of 1.726 Å are in good agreement with the experimental result of 1.794 Å. The calculated and experimental geometries (given in parentheses) for the ***s*** model, which belongs to the orthorhombic space group *Pnca*, consist of lattice parameters and unit cell volume: a = 8.991 (**9.1386**) Å; b = 12.343 (**12.6234**) Å and c = 8.942 (**9.0438**) Å; and V = 992.29 (**1043.29**)$Å^3$. The orthorhombic structure in ***s**** state expanded somewhat in the three directions of the crystal. There is an expansion of tetrahedral

[$W1O_4$] clusters while a distortion of tetrahedral [$W2O_4$] more noticeable in ***s**** state compared to the ground state (Supplementary data Figs S3). Based on our theoretical results, total energy variation between ***s**** and ***s*** states is 0.35 eV.

3.3. Electronic structure and UV–visible absorption spectroscopy analyses of $Al_2(WO_4)_3$ crystals

The optical band gap energy (E_{gap}) was calculated by the method proposed by Kubelka and Munk [**47**] which is based on transformation of diffuse reflectance measurements to estimate E_{gap} values with good accuracy within the limits of assumptions when modeled in three dimensions [**48**]. Particularly, it is useful in limited cases of an infinitely thick sample layer. The Kubelka–Munk equation for any wavelength is described by Eq. (**2**):

$$\frac{K}{S} = \frac{(1 - R_\infty)^2}{2R_\infty} \equiv F(R_\infty) \quad (2)$$

where $F(R_\infty)$ is the Kubelka–Munk function or absolute reflectance of the sample. In our case, magnesium oxide (MgO) was the standard sample in reflectance measurements. $R_\infty = R_{sample}/R_{MgO}$ (R_∞ is the reflectance when the sample is infinitely thick), k is the molar absorption coefficient and s is the scattering coefficient. In a parabolic band structure, the optical band gap and absorption coefficient of semiconductor oxides [**49**] can be calculated by Eq. (**3**):

$$\alpha h\nu = C_1(h\nu - E_{gap})^n \quad (3)$$

where α is the linear absorption coefficient of the material, $h\nu$ is the photon energy, C_1 is a proportionality constant, E_{gap} is the optical band gap and n is a constant associated with different kinds of electronic transitions (n = 0.5 for a direct allowed, n = 2 for an indirect allowed, n = 1.5 for a direct forbidden and n = 3 for an indirect forbidden). According to the

literature [**50**–**54**], tungstate crystals exhibit an optical absorption spectrum governed by direct or indirect electronic transitions.

The band structure and DOS projected were calculated for the both $Al_2(WO_4)_3$ models and the results are illustrated in Figs. 3(a–d).

<Figs. 3(a–d)>

An analysis of the band structure displayed in Figs. 3(a,b) show that the band gap values are indirect ($\Gamma \rightarrow Z$) and direct ($\Gamma \rightarrow \Gamma$) transitions for ***s*** and ***s**** models, respectively. A noticeable decrease of the band gap energy from going to fundamental ***s*** (6.16 eV) to exited ***s**** (5.84 eV) electronic state is sensed. An analysis of the DOS projected on atoms and orbitals for the ***s*** and ***s**** models presented in Figs. 3(c,d) indicate that uppermost levels in the VB consist mainly of O 2*p* orbitals with a lower contribution of W 5*d* and Al 4*s* orbitals, while the CB is formed mainly by the W 5*d* and O 2*p* orbital states with a small contribution of Al 4*s* orbitals. The distortion process from the fundamental to excited tetrahedral [WO_4] clusters provokes the decrease of the band gap value, and we sense a difference between the atomic orbital contributions in ***s*** and ***s**** models, in particular for the W *5d* orbitals. Our findings suggest an increase in the contribution of the W atoms related to $5d_{xy}$ and $5d_{yz}$ orbitals levels in ***s**** state compared to the ground state, and thus they have a more important role for the PL behavior of $Al_2(WO_4)_3$ powders.

An analysis of site- and orbital-resolved DOS shows a significant dependence of the W CB DOS's on the local coordination. During the excitation process some electrons are promoted more feasibly from the O 2*p* states to the W5*d* states in ($5d_{xy}$ and $5d_{yz}$ orbitals) through the absorption of photons. These results show that the properties of this material are strongly influenced by the degree of structural order-disorder, which provides a change in the

transition from indirect-to-direct band gap at fundamental ***s*** and excited, ***s****, electronic states, respectively. The changes result in a decrease of the band gap energy for the $Al_2(WO_4)_3$ powders.

Based on this theoretical information for the ***s*** model, E_{gap} values of $Al_2(WO_4)_3$ powders were calculated using $n = 0.5$. Finally, using the remission function described in **Eq. 3** with $k = 2\alpha$, we obtain the modified Kubelka–Munk equation as indicated **in Eq. (4):**

$$[F(R_\infty)h\nu)^2 = C_2(h\nu - E_{gap}) \quad \ldots\ldots\ldots\ldots\ldots\ldots\ldots\ldots\ldots\ldots\ldots\ldots\ldots\ldots (4)$$

Therefore, finding the $F(R_\infty)$ value from Eq. (**4**) and plotting a graph of $[F(R_\infty)h\nu]^2$ against $h\nu$, we can determine the E_{gap} values for our $Al_2(WO_4)_3$ powders with greater accuracy by extrapolating the linear portion of the UV–vis curves. In general, different types of defects generated during the synthesis enable a change in its optical transitions offering an opportunity to tune their properties by the band gap engineering.

Figs. 4(a–e) show UV–vis spectra for $Al_2(WO_4)_3$ powders heat-treated at 100, 200, 400ºC, 800ºC and 1000°C for 2 h.

<Figs. 4(a–e)>

Evidently, powders have different E_{gap} values which are possibly related to the existence of new energy levels near the CB, which were confirmed by theoretical calculations. The E_{gap} value is low (from 3.16 to 3.48 eV) for $Al_2(WO_4)_3$ powders heat-treated at 100 ºC, 200ºC and 400ºC for 2 h (see Figs. 4(a–c)) which indicates a high defect concentration and intermediate levels between the VB and CB for these powders. However, for $Al_2(WO_4)_3$ powders heat-treated at 800ºC and 1000ºC for 2 h, we observed typical absorption spectra for crystalline materials or an ordered structure (see Figs. 4(d,e)).

We have performed an analysis of the charge density contour for the **single (*s*) and excited single (*s**) models**, as illustrated in Figs. 5(a**,b**). These electronic density maps were performed to provide a deep insight into the molecular geometry, symmetry breaking and electronic order-disorder effects.

<Figs. 5(a,b)>

Our **theoretical results** reveal a possible **hybridization between 5d (W) and 2p (O) linked to (W–O) bond presents in tetrahedral [WO_4] clusters. A displacement of W atoms from the ideal center in tetrahedral [WO_4] clusters was performed to represent** the ***s*** model. **These electronic perturbations promote an increase in the charge density on the atomic sites forming the trigonal pyramidal** [$WO_3.V_O^z$] clusters, which are assigned ***s**** model, as can be viewed in Figs. 5(a,b)). **These theoretical calculated results indicate the possible effects** on their structure and electronic properties that involves the presence of the ***s**** **in disordered lattice**, which could be the main responsible of PL behavior in disordered $Al_2(WO_4)_3$ powders.

4.4. PL emission analyses of $Al_2(WO_4)_3$ powders

Fig. 6(a–e) illustrate the PL emission spectra at room temperature of $Al_2(WO_4)_3$ powders obtained by coprecipitation and heat-treated at different temperatures for 2 h.

<Fig. 6(a–e)>

Blasse and Ouwerkerk [18] have been proposed that PL properties of $Al_2(WO_4)_3$ crystals are related to self-localized excitons and electronic transitions within the two types of tetrahedral [WO_4] clusters in their crystal structure, while Kotlov *et al*. **[55]** suggested that free electrons and holes are created in this material due to electronic transitions from oxygen to cation states which are situated several electron volts above the bottom of the CB. In this research, we have observed a highly intense PL emission at room temperature. Based on our structural and electronic investigations, we ascribe this PL behavior to structural and electronic order-disorder effects of tetrahedral [WO_4] clusters in $Al_2(WO_4)_3$ powders. Our theoretical results suggest that structural and electronic order-disorder effects cause a polarization of one type of **tetrahedral** [WO_4] clusters that facilitates the population of electronic excited states, and they may return to lower energy and fundamental states via radiative and/or non-radiative relaxations, which promotes a intense PL emission in $Al_2(WO_4)_3$ powders.

5. Conclusions

In summary, $Al_2(WO_4)_3$ powders were synthesized by the CP method at room temperature without surfactants and heat-treated at different temperatures for 2 h. XRD patterns indicate that crystalline $Al_2(WO_4)_3$ powders obtained by the CP method and **heat-treated** at 800ºC and 1000ºC have an orthorhombic structure with a space group *Pnca*. FE-SEM images revealed large particles **for** crystalline $Al_2(WO_4)_3$ powders with irregular shapes. Particle growth is related to mass transport mechanisms via nanocrystalline particle diffusion during the sintering process by an increase of the heat treatment. UV-vis spectra show an increase in the optical band gap with a calcination temperature which raise and suggest a direct allowed transition with the existence of intermediary energy levels between the VB and CB. Stable electronic excited states (singlet) have been characterized by using DFT method at

the B3LYP calculation level of model. The analysis of the band structures and density of states of both ground and first excited electronic states allows a deep insight on the main electronic features based on structural and electronic order-disorder effects of both octahedral [AlO_6] and tetrahedral [WO_4] clusters, as constituent building units of this material. These findings confirm that PL is directly associated with structural and electronic order-disorder effects on one type of tetrahedral [WO_4] clusters that facilitates the population of electronic excited states and provides new insight into PL behaviour in these materials. Present results offers new ideas and perspectives on the behavior of **optical** materials and the results suggest that these materials are promising for applications in photovoltaic devices and catalysis.

Acknowledgments

The Brazilian authors acknowledge the financial support of the Brazilian research financing institutions: CNPq (304531/2013-8), FAPESP (09/50303-4; 12/18597-0), and CAPES. The Spanish authors would like to thank the Spanish Government MAT2010-21088-C03 project and the Catalan Government PIGC project 2009-SGR-0674. J. Andrés acknowledges Generalitat Valenciana (Prometeo/2009/053 project), Ministerio de Ciencia e Innovación (CTQ-2012-36253-C03-01) Programa de Cooperación Científica con Iberoamerica (Brazil), Ministerio de Educación (PHB2009-0065-PC project).

Appendix A. Supplementary data

Supplementary data associated with this article can be found in the attached files.

References

[1] G.D. Mukherjee, S.N. Achary, A.K. Tyagi, S.N. Vaidya, *J. Phys. Chem. Solids.* 64 (2003) 611–614.

[2] N. Garg, V. Panchal, A.K. Tyagi, S.M. Sharma, *J. Solid State Chem.* 178 (2005) 998–1002.

[3] V. Sivasubramanian, T.R. Ravindran, S. Kalavathi, A.K. Arora, *J. Electroceram.* 17 (2006) 57–60.

[4] M. Maczka, V. Nikolov, K. Hermanowicz, A. Yordanova, M. Kurnatowska, J. Hanuza, *Opt. Mater*. 34 (2012) 1048–1053.

[5] J.J. de Boer. *Acta Cryst*. B 30 (1974) 1878–1880.

[6] J. Hanuza, M. Maczka, K. Hermanowicz, M. Andruszkiewicz, A. Pietraszko, W. Strek, P. Dereń, *J. Solid State Chem*. 105 (1993) 49–69.

[7] K. Nassau, H.J. Levinstein, G.M. Loiacono, *J. Phys. Chem. Solids.* 26 (1965) 1805–1816.

[8] I. Koseva, A. Yordanova, P. Tzvetkov, V. Nikoloa, D. Nihtianova, *Mater. Chem. Phys.* 132 (2012) 808–814.

[9] D. Nihtianova, N. Velichkova, R. Nikolova , I. Koseva , A. Yordanova , V. Nikolov, *Mater. Res. Bull.* 46 (2011) 2125–2130.

[10] D. C. Craig, N.C. Stephenson, *Acta Crystallogr. B.* 24 (1968) 1250–1255.

[11] K. Nassau, H.J. Levinstein, G.M. Loiacono, *J. Phys. Chem. Solids* 26 (1965) 1805–1816.

[12] A. Yordanova, I. Koseva, N. Velichkova, D. Kovacheva, D. Rabadjieva, V. Nikolov, *Mater. Res. Bull.* 47 (2012) 1544–1549.

[13] E. Zhecheva, R. Stoyanova, S. Ivanova, V. Nikolov, *Solid State Sci*. 12 (2010) 2010–2014.

[14] V. Nikolov, I. Koseva, R. Stoyanova, E. Zhecheva, *J. Alloys Compd*. 505 (2010) 443–449.

[15] I.I. Koseva, V. S. Nikolov, *Bulg. Chem. Commun.* 42 (2010) 300–304.

[16] E. Gallucci, S. Ermeneux, C. Goutaudier, M. Th. Cohen-Adad, G. Boulon, *Opt. Mater*. 16 (2004) 193–197.

[17] N. Imanaka, S. Tamura, M. Hiraiwa, G. Adachi, *Chem. Mater*. 10 (1998) 2542–2545

[18] G. Blasse, M. Ouwerkerk, *J. Electrochem. Soc*. 127 (1980) 429–434.

[19] I. Nikolov , X. Mateos , F. Guell, J. Massons, V. Nikolov , P. Peshev, F.Díaz, *Opt. Mater*. 25 (2004) 53–58.

[20] G. D. Mukherjee, V. Vijaykumar, S. N. Achary, A. K. Tyagi, B. K.Godwal1, *J. Phys. Condens. Matter* 16 (2004) 7321–7330.

[21] D. Nihtianova, N. Velichkova, R. Nikolova, I. Koseva, A. Yordanova, V. Nikolov, *Mater. Res. Bulletin* 46 (2011) 2125–2130.

[22] J.S.O. Evans, T.A. Mary, A.W. Sleight, *J. Solid State Chem*. 133 (1997) 580–583.

[23] T.A. Mary, A.W. Sleight, *J. Mater. Res*. 14 (1999) 912–915.

[24] T. Sugimoto, Y. Aoki, E. Niwa, T. Hashimoto, Y. Morito, *J. Ceram. Soc. Jpn*. 115 (2007) 176–181.

[25] C. Lind, *Materials*. 5 (2012) 1125–1154.

[26] R.J. Speedy, *J. Phys.: Condens. Matter* 8 (1996) 10907–10918.

[27] T.A. Mulinari, F.A. La Porta, J. Andrés, M. Cilense, J.A. Varela, E. Longo, *CrystEngComm*. 15 (2013) 7443–7449.

[28] L.S. Cavalcante, F.M.C. Batista, M.A.P. Almeida, A.C. Rabelo, I.C. Nogueira, N.C. Batista, J. A. Varela, M.R.M.C. Santos, E. Longo, M. Siu Li, *RSC Adv*. 2 (2012) 6438–6454.

[29] F.A. La Porta, M.M. Ferrer, Y.V.B. Santana, C.W. Raubach, V.M. Longo, J.R. Sambrano, E. Longo, J. Andrés, M. S. Li, J. A. Varela, *J. Alloys Compd.* 555 (2013) 153–159.

[30] A.D. Becke, *J. Chem. Phys.* 98 (1993) 5648–5653.

[31] C. Lee, W. Yang, R.G. Parr, *Phys. Rev. B.* 37 (1988) 785–789.

[32] R. Dovesi, V.R. Saunders, C. Roetti, R. Orlando, C.M. Zicovich-Wilson, F. Pascale, B. Civalleri, K. Doll, N.M. Harrison, I.J. Bush, P.D. Arco, M. Llunell, CRYSTAL09 Users Manual, University of Torino, 2009.

[33] P.J. Hay, W.R. Wadt, *J. Chem. Phys.* 82 (1985) 299–310.

[34] Available at: < http://www.crystal.unito.it/Basis_Sets/Ptable.html>.

[35] H.J. Monkhorst, J.D. Pack, *Phys. Rev.* 13 (1976) 5188–5192.

[36] I. Gadaczek, K. J. Hintze, T. Bredow, *Phys. Chem. Chem. Phys.* 14 (2012) 741–750.

[37] L. Gracia, J. Andres, V.M. Longo, J.A. Varela, E. Longo, *Chem. Phys. Lett.* 493 (2010) 141–146.

[38] M.L. Moreira, J. Andres, L. Gracia, A. Beltrán, L.A. Montoro, J.A. Varela, E. Longo, *J. Appl. Phys*. 114 (2013) 043714–043722.

[39] L. Gracia, V.M. Longo, L.S. Cavalcante, A. Beltran, W. Avansi, M.S. Li, V.R. Mastelaro, J.A. Varela, E. Longo, J. Andres, *J. Appl. Phys*. 110 (2011) 043501–043511.

[40] M.R.D. Bomio, R.L. Tranquilin, F.V.Motta, C.A. Paskocimas, R.M. Nascimento, L. Gracia, J. Andres, E. Longo, *J. Phys. Chem. C* 117 (2013) 21382−21395.

[41] A. Kokalj, *J. Mol. Graphics. Modell.* 17 (1999) 176−179.

[42] D.A. Woodcock, P. Lightfoot, C. Ritter, *J. Solid State Chem*. 149 (2000) 92–98.

[43] H.M. Rietveld. J. Appl. Cryst. 2 (1969) 65–71.

[44] M. Bortolotti, L. Lutterotti, I. Lonardelli, J. Appl. Cryst. 42 (2009) 538-539.

[45] K. Momma, F. Izumi, *J. Appl. Crystallogr*. 44 (2011) 1272–1276.

[46] J. S. O. Evans, T.A. Mary, A.W. Sleight, *J. Solid State Chem*. 137 (1998) 148–160.

[47] W. Paraguassu, M. Maczka, A.G. Souza Filho, P.T.C. Freire, F.E.A. Melo, J. Mendes Filho, J. Hanuza, *Vib. Spectrosc.* 44 (2007) 69–77.

[48] P. Kubelka, F. Munk-Aussig, *Zeit. Für. Tech. Physik*. 12 (1931) 593–601.

[49] A.E. Morales, E.S. Mora, U. Pal, *Rev. Mex. Fis. S*. 53 (2007) 18–22.

[50] R.A. Smith, Semiconductors, 2nd ed.; Cambridge University Press: London, (1978); p 434.

[51] R. Lacomba-Perales, J. Ruiz-Fuertes, D. Errandonea, D. Martínez-García, A. Segura, *Eur. Phys. Lett*. 83 (2008) 37002–37006.

[52] L.S. Cavalcante, M.A.P. Almeida, W. Avansi, R.L. Tranquilin, E. Longo, N.C. Batista, V.R. Mastelaro, M. Siu Li, *Inorg. Chem*. 51 (2012) 10675–10687.

[53] L.S. Cavalcante, V.M. Longo, J.C. Sczancoski, M.A.P. Almeida, A.A. Batista, J.A. Varela, M.O. Orlandi, E. Longo, M. Siu Li, *CrystEngComm*. 14 (2012) 853–868.

[54] E.I. Ross-Medgaarden, I. E. Wachs, *J. Phys. Chem. C.* 111 (2007) 15089–15099.

[55] A. Kotlov, S. Dolgov, E. Feldbach, L. Jönsson, M. Kirm, A. Lushchik, V. Nagirnyi, G. Svensson, B.I. Zadneprovski, *Phys. Stat. Sol. C*. 2 (2005) 61–64.

Figures Captions:

Fig. 1(a–e): XRD patterns for the $Al_2(WO_4)_3$ powders heat-treated **(a)** 100°C, **(b)** 200°C, **(c)** 400°C, **(d)** 800°C and **(e)** 1000°C for 2 h, respectively.

Fig. 2: Schematic representation of the orthorhombic unit cells corresponding to $Al_2(WO_4)_3$ crystals.

Fig. 3: (a-b) Band structures and (c–d) projected DOS on atomic levels for both o-$Al_2(WO_4)_3$ and d-$Al_2(WO_4)_3$ models.

Fig. 4: UV–vis spectra for the $Al_2(WO_4)_3$ powders heat-treated at: **(a)** 100°C, **(b)** 200°C, **(c)** 400°C, **(d)** 800°C and **(e)** 1000°C for 2 h, respectively.

Fig. 5: Charge density maps in **(a)** ordered and **(b)** disordered $Al_2(WO_4)_3$ models.

Fig. 6: PL emission spectra for the $Al_2(WO_4)_3$ powders heat-treated at **(a)** 100°C, **(b)** 200°C, **(c)** 400°C, **(d)** 800°C and **(e)** 1000°C for 2 h, respectively.

Table Captions:

Tab. 1: Optimized lattice parameters, **bond distances and angles bonds [(Al–O); (W1–O); (W2–O)] for the singlet** (*s*) and excited singlet (*s**) electronic states.

Highlights

- $Al_2(WO_4)_3$ powders were obtained by the coprecipitation/calcination methods
- Rietveld refinement data were employed to $[AlO_6]/[WO_4]$ clusters modeling
- Electronic structure of $Al_2(WO_4)_3$ was performed by the density functional theory
- A correlation between the theoretical and experimental optical band gap was observed
- Singlet excited state is very important to photoluminescence properties of $Al_2(WO_4)_3$

Figures:

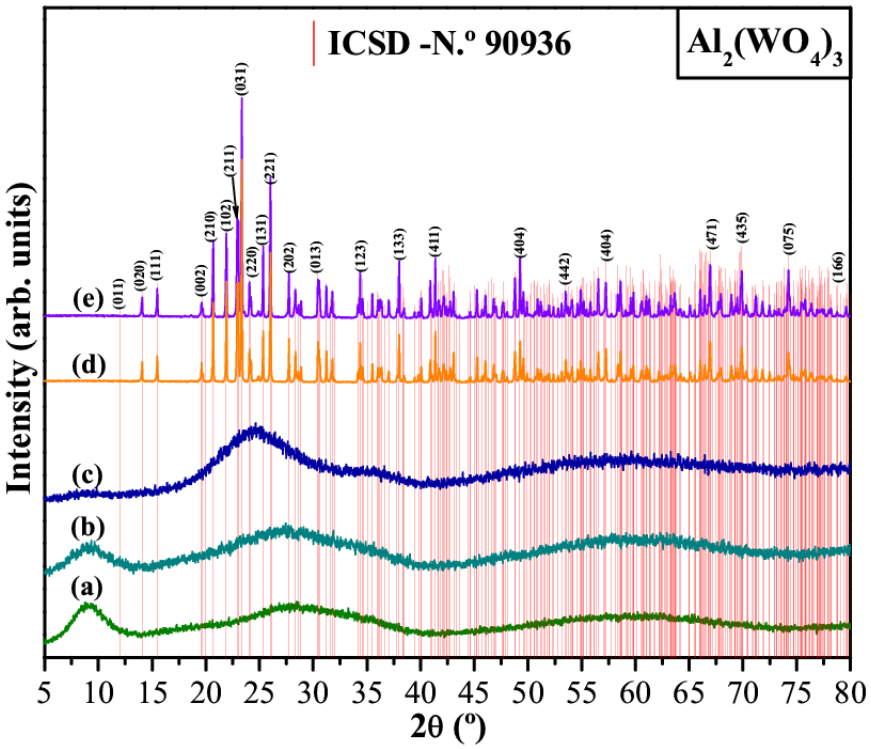

<Fig. 1(a-e)>

a)

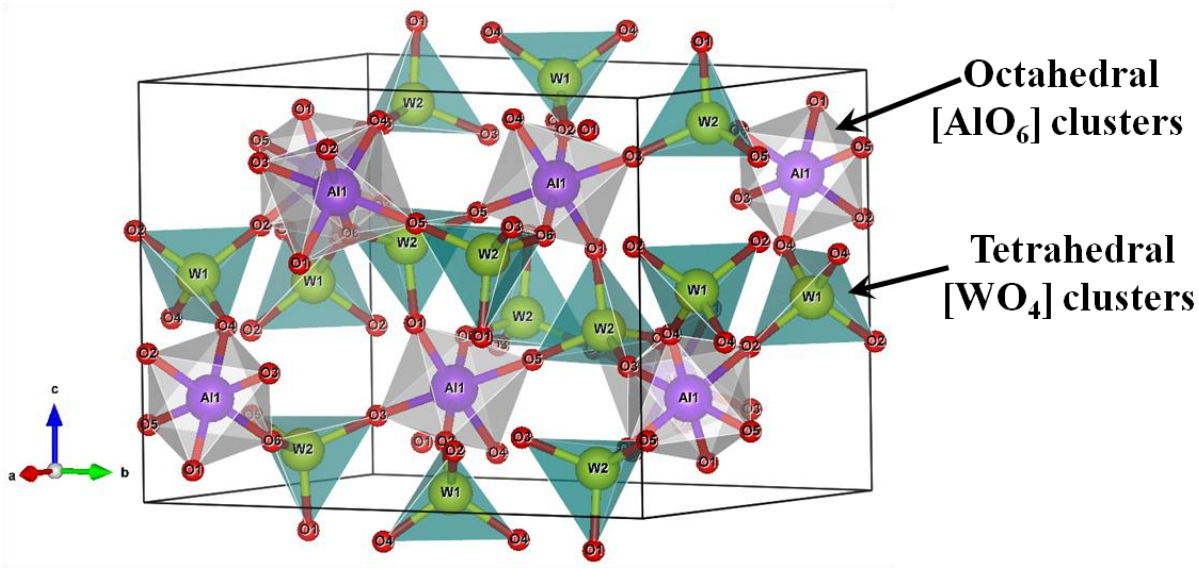
Octahedral
[AlO6] clusters
Tetrahedral
[WO4] clusters
c
a
b
Al1
W1
W2
O1
O2
O3
O4
O5

<Fig. 2>

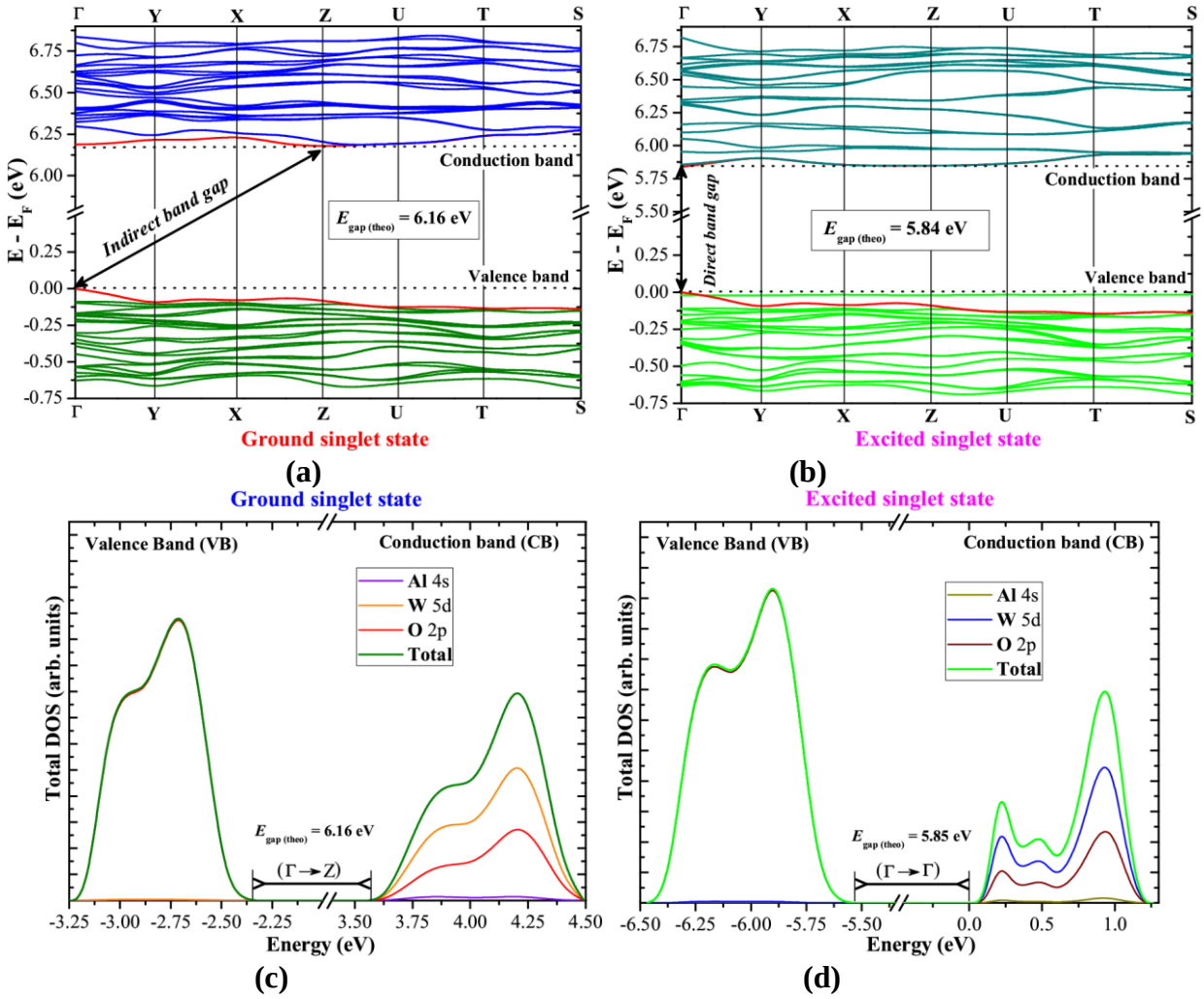
Γ Y X Z U T S
E - E_F (eV)
Conduction band
Valence band
Indirect band gap
E_gap (theo) = 6.16 eV
Ground singlet state
(a)
Direct band gap
E_gap (theo) = 5.84 eV
Excited singlet state
(b)
Ground singlet state
Valence Band (VB)
Conduction band (CB)
Al 4s
W 5d
O 2p
Total
Total DOS (arb. units)
E_gap (theo) = 6.16 eV
(Γ → Z)
Energy (eV)
(c)
Excited singlet state
E_gap (theo) = 5.85 eV
(Γ → Γ)
(d)

<Figs. 3(a–d)>

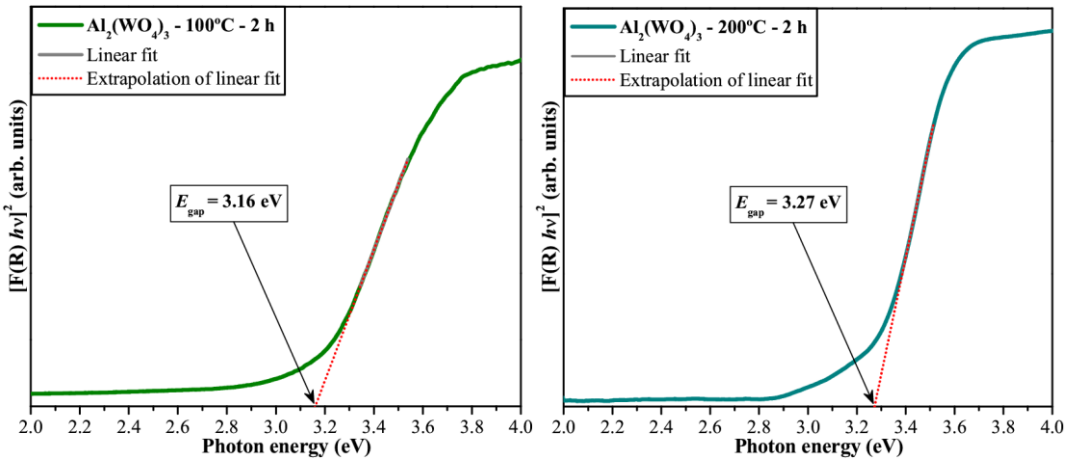

(a)

(b)

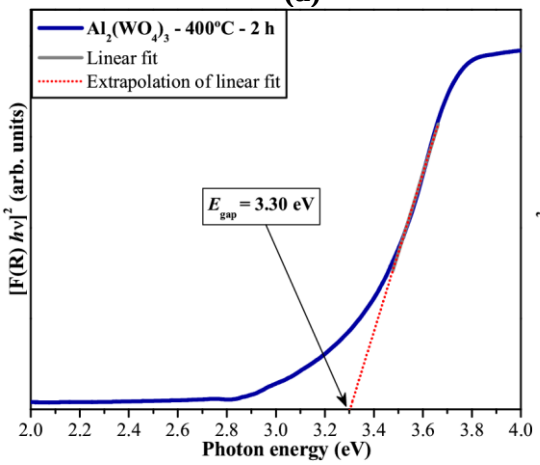

(c)

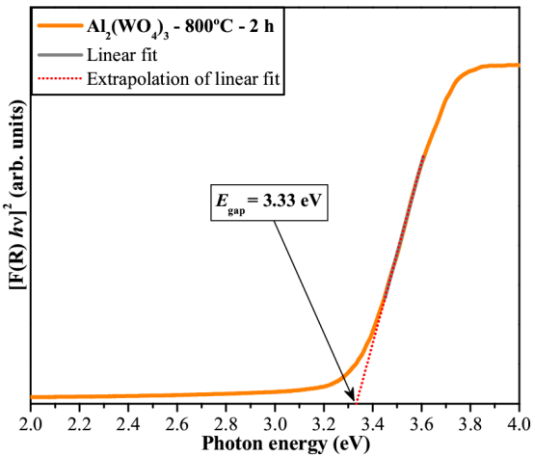

(d)

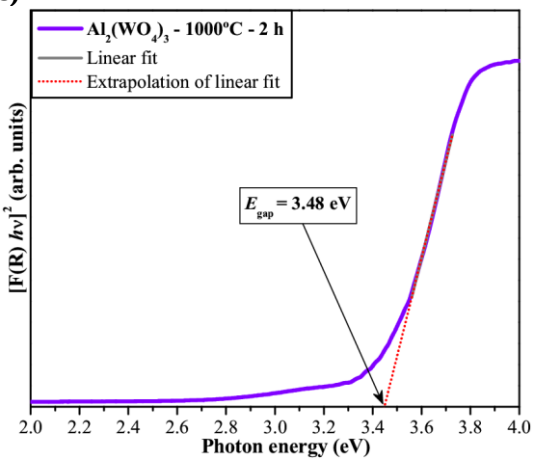

(e)

<Figs. 4(a–e)>

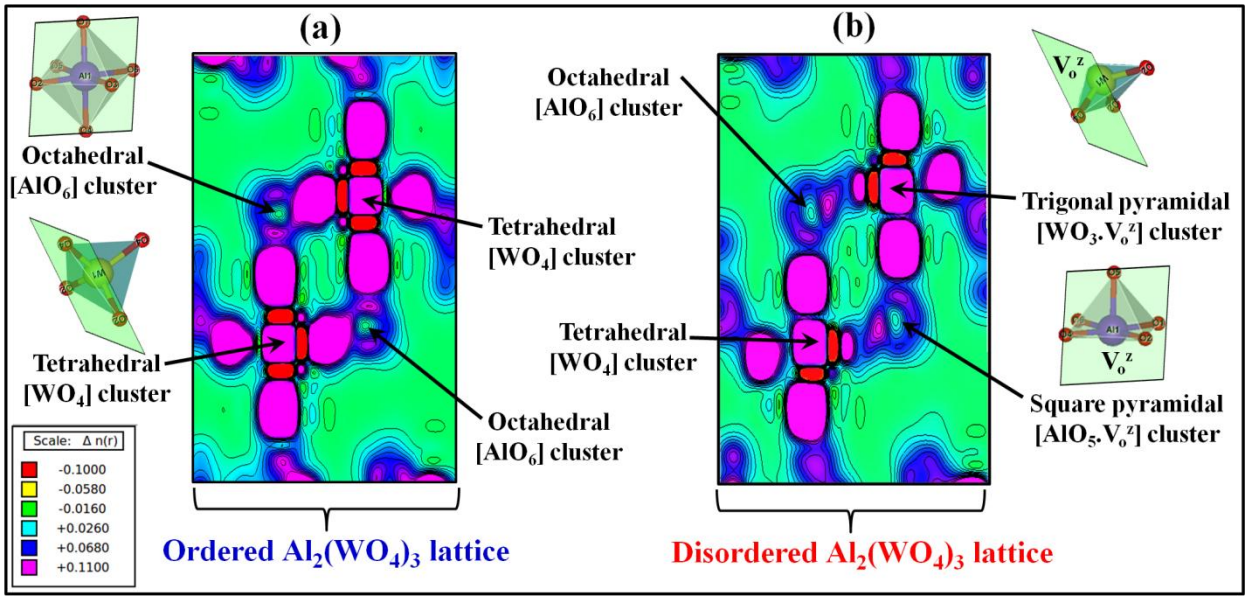
(a)
(b)
Octahedral
[AlO6] cluster
Tetrahedral
[WO4] cluster
Octahedral
[AlO6] cluster
Tetrahedral
[WO4] cluster
Scale: Δ n(r)
-0.1000
-0.0580
-0.0160
+0.0260
+0.0680
+0.1100
Ordered Al2(WO4)3 lattice
Octahedral
[AlO6] cluster
Tetrahedral
[WO4] cluster
Trigonal pyramidal
[WO3.Vo z] cluster
Square pyramidal
[AlO5.Vo z] cluster
Disordered Al2(WO4)3 lattice

<Figs. 5(a,b)>

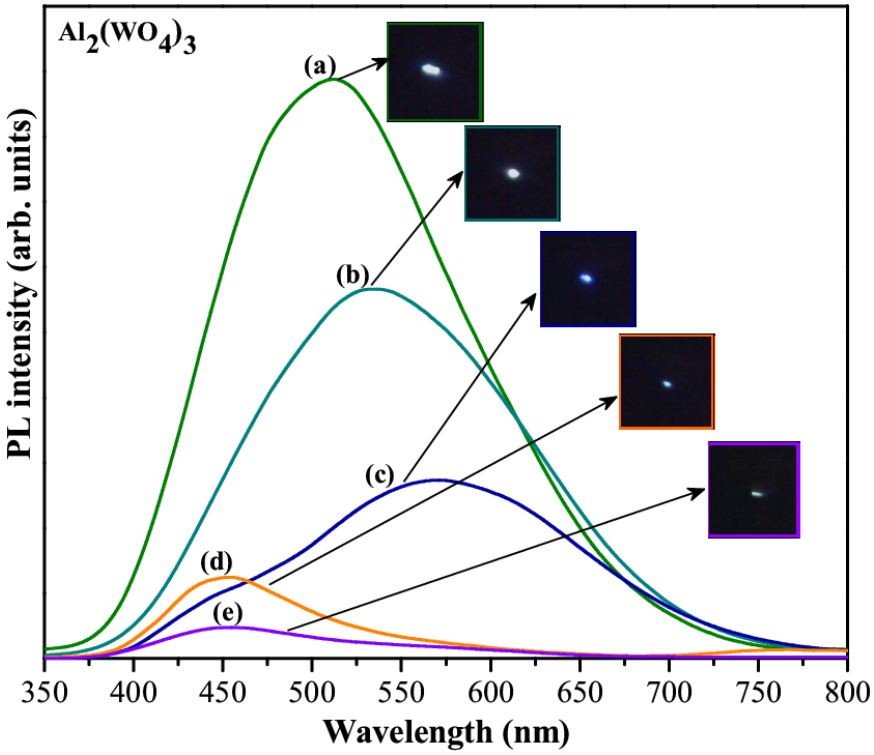
$Al_2(WO_4)_3$
(a)
(b)
(c)
(d)
(e)
PL intensity (arb. units)
350
400
450
500
550
600
650
700
750
800
Wavelength (nm)

<Fig. 6(a–e)>

A joint experimental and theoretical study on the electronic structure and photoluminescence properties of $Al_2(WO_4)_3$ powders

F.M.C. Batista[a], F.A. La Porta[b,c], L. Gracia[b,c], E. Cerdeiras[a], L. Mestres[a], M. Siu Li[d], N.C. Batista[e], J. Andrés[b], E. Longo[c], L.S. Cavalcante[e*]

[a]*Departament de Química Inorgànica, Facultat de Química, Universitat de Barcelona, 08028 Barcelona, Spain*
[b]*Departament de Química Física i Analítica, UJI – Universitat Jaume I, Av. de Vicent Sos Baynat, s/n, Castelló de la Plana, 12071, Spain*
[c]*Universidade Estadual Paulista, P.O. Box 355, 14801-907, Araraquara-SP, Brazil*
[d]*IFSC-Universidade de São Paulo, P.O. Box 369, 13560-970, São Carlos, SP, Brazil*
[e]*CCN-DQ-GERATEC, Universidade Estadual do Piauí; João Cabral, N. 2231, P.O. Box 381, CEP: 64002-150, Teresina-PI, Brazil*

Abstract Graphical

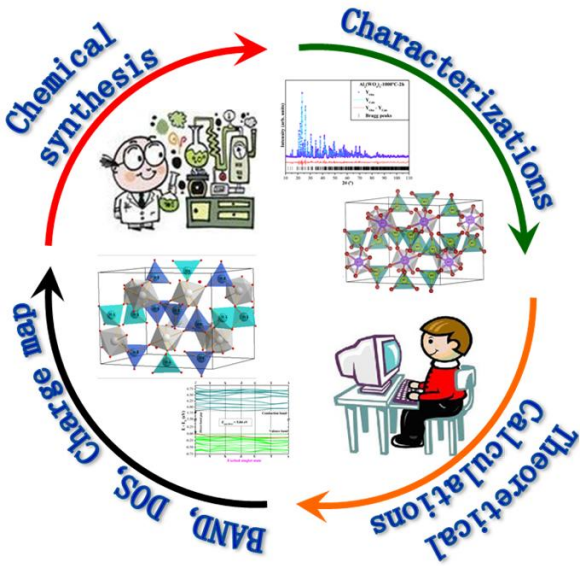

Tables:

Table 1.

$Al_2(WO_4)_3$ lattice	Singlet (*s*)	Excited singlet (*s**)
a	8.991	9.011
b	12.343	12.402
c	8.942	9.000
Al−O	1.870(1), 1.876(1), 1.888(1)	1.874(1), 1.876(1), 1.878(1)
	1.894(1), 1.911(1), 1.932(1)	1.892(1), 1.899(1), 1.936(1)
W1−O	1.726(2), 1.730(2)	1.748(2), 1.752(2)
W2−O	1.726(2), 1.731(1), 1.733(1)	1.726(1), 1.731(1), 1.734(1), 1.736(1)

A joint experimental and theoretical study on the electronic structure and photoluminescence properties of $Al_2(WO_4)_3$ powders

F.M.C. Batista[a], F.A. La Porta[b,c], L. Gracia[b,c], E. Cerdeiras[a], L. Mestres[a], M. Siu Li[d], N.C. Batista[e], J. Andrés[b], E. Longo[c], L.S. Cavalcante[e*]

[a]*Departament de Química Inorgànica, Facultat de Química, Universitat de Barcelona, 08028 Barcelona, Spain*
[b]*Departament de Química Física i Analítica, UJI – Universitat Jaume I, Av. de Vicent Sos Baynat, s/n, Castelló de la Plana, 12071, Spain*
[c]*Universidade Estadual Paulista, P.O. Box 355, 14801-907, Araraquara-SP, Brazil*
[d]*IFSC-Universidade de São Paulo, P.O. Box 369, 13560-970, São Carlos, SP, Brazil*
[e]*CCN-DQ-GERATEC, Universidade Estadual do Piauí; João Cabral, N. 2231, P.O. Box 381, CEP: 64002-150, Teresina-PI, Brazil*

Supplementary data:

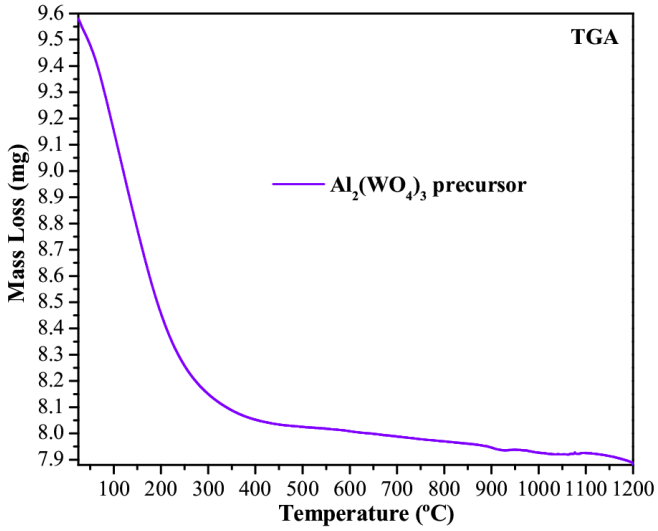

(a)

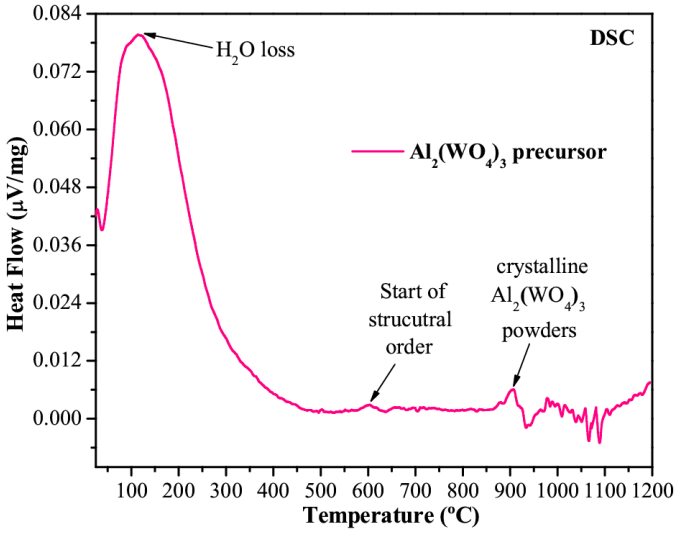

(b)

Figs S1(a,b): TGA/DSC curves of the dried $Al_2(WO_4)_3$ powders.

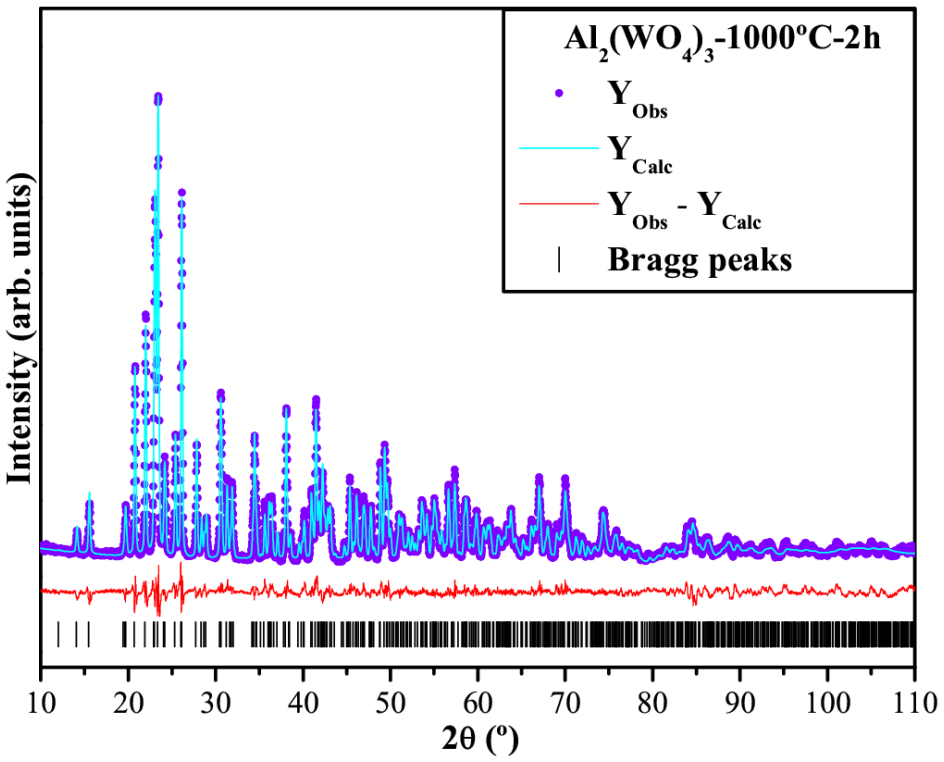

Figs S2: Rietveld refinement plot of $Al_2(WO_4)_3$ powders **heat–treated at 1000ºC** for 2 h.

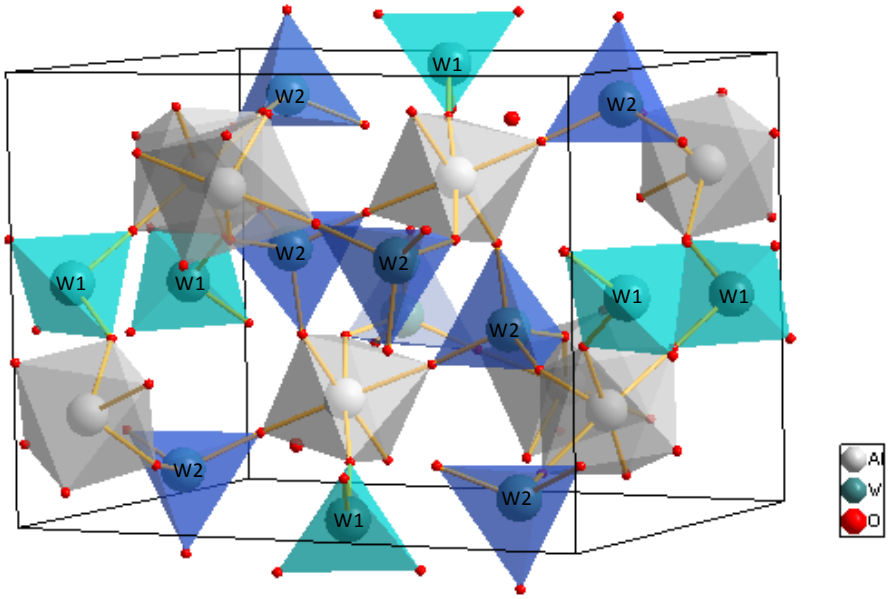

Figs S3: Schematic representation of the orthorhombic unit cells which was theoretically modeled by optimization of lattice and atomic positions.

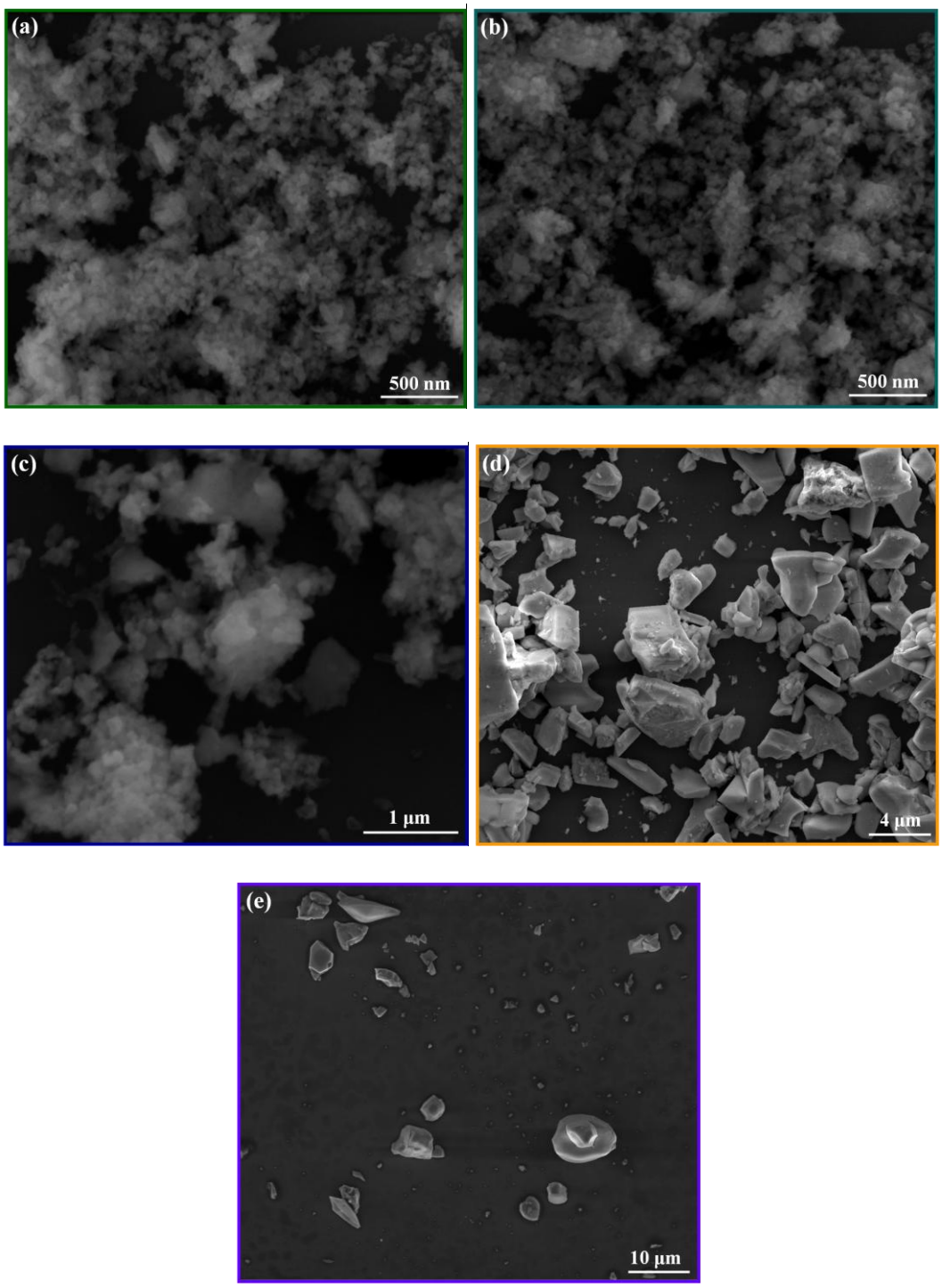

Figs. S4(a–e): FE-SEM images for $Al_2(WO_4)_3$ powders heat-treated at 100, 200, 400, 800 and 1000ºC for 2 h, respectively.

Table S1: Lattice parameters, unit cell volume, atomic coordinates and site occupation obtained by Rietveld refinement data for the $Al_2(WO_4)_3$ powders obtained by the CP method and heat-treated at 1000 ºC for 2 h.

Atoms	Wyckoff	Site	*x*	*y*	*z*
Al1	8*d*	1	**0.46688**	**0.37988**	**0.24988**
W1	4*c*	.2.	**0.25**	**0**	**0.475**
W2	8*d*	1	**0.11665**	**0.35711**	**0.39485**
O1	8*d*	1	**0.09251**	**0.14131**	**0.09122**
O2	8*d*	1	**0.13115**	**0.07878**	**0.37411**
O3	8*d*	1	**0.00621**	**0.25822**	**0.31721**
O4	8*d*	1	**0.34466**	**0.37083**	**0.07452**
O5	8*d*	1	**0.06687**	**0.50029**	**0.33315**
O6	8*d*	1	**0.31452**	**0.34125**	**0.36121**

a = **9.1386(2)** Å, *b* = **12.6234(5)**Å, *c* = **9.0438(2)**Å; *V* = **1043.29(5)**Å^3; Z = 4

R_p **= 6.54%;** R_{exp} **= 4.42%;** R_{wp} **= 8.71%;** χ^2 **= 3,94;** ***GoF*** **= 1.97**